Landes Bioscience www.landesbioscience.com

Supplemental Material to:

Bin Guo, Jie Huang, Wenxian Wu, Du Feng, Xiaochen Wang, Yingyu Chen, and Hong Zhang

The nascent polypeptide-associated complex is essential for autophagic flux

Autophagy 2014; 10(10)
http://dx.doi.org/10.4161/auto.29638

www.landesbioscience.com/journals/autophagy/article/29638

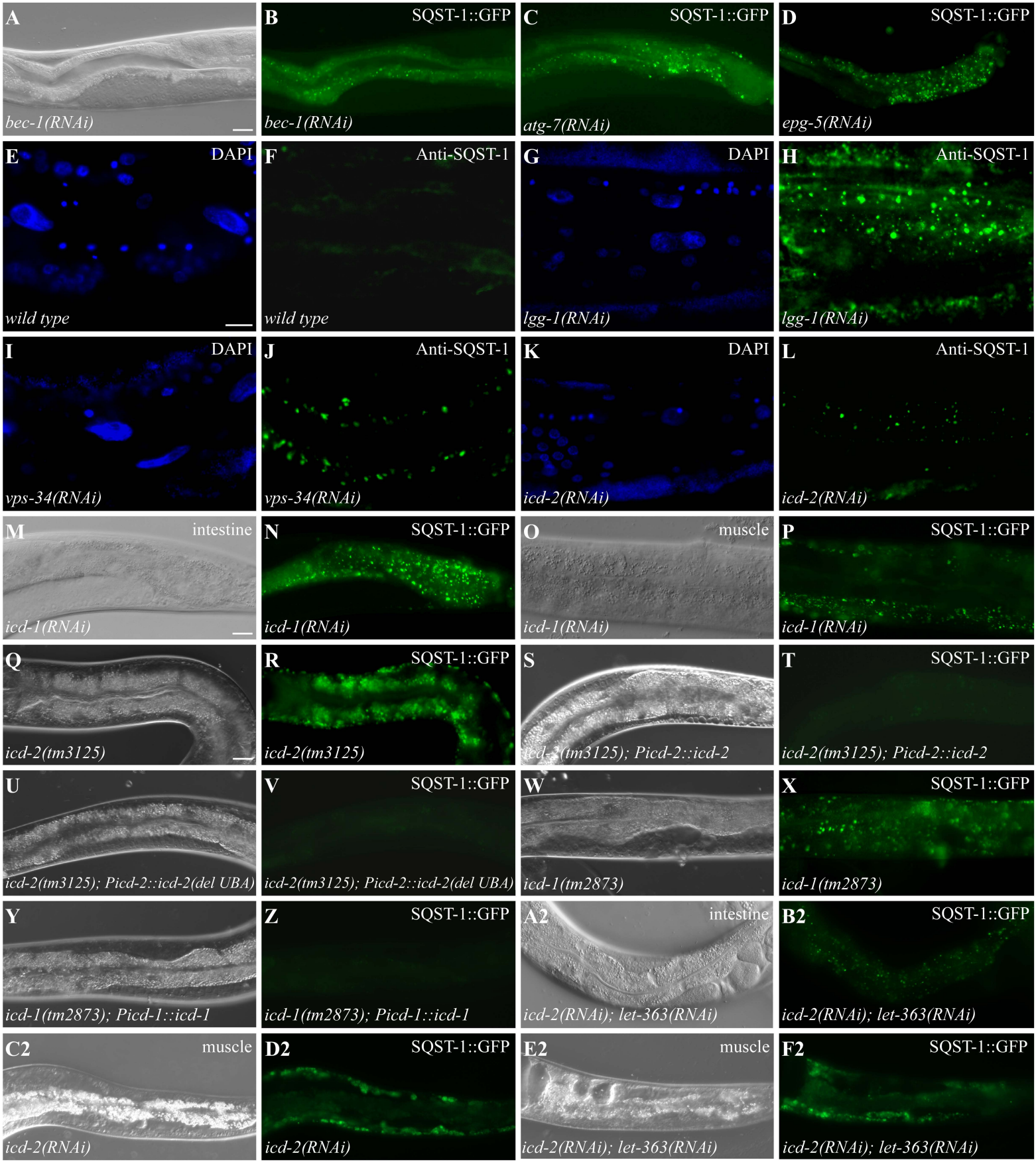
A
bec-1(RNAi)
B
SQST-1::GFP
bec-1(RNAi)
C
SQST-1::GFP
atg-7(RNAi)
D
SQST-1::GFP
epg-5(RNAi)
E
DAPI
wild type
F
Anti-SQST-1
wild type
G
DAPI
lgg-1(RNAi)
H
Anti-SQST-1
lgg-1(RNAi)
I
DAPI
vps-34(RNAi)
J
Anti-SQST-1
vps-34(RNAi)
K
DAPI
icd-2(RNAi)
L
Anti-SQST-1
icd-2(RNAi)
M
intestine
icd-1(RNAi)
N
SQST-1::GFP
icd-1(RNAi)
O
muscle
icd-1(RNAi)
P
SQST-1::GFP
icd-1(RNAi)
Q
icd-2(tm3125)
R
SQST-1::GFP
icd-2(tm3125)
S
icd-2(tm3125); Picd-2::icd-2
T
SQST-1::GFP
icd-2(tm3125); Picd-2::icd-2
U
icd-2(tm3125); Picd-2::icd-2(del UBA)
V
SQST-1::GFP
icd-2(tm3125); Picd-2::icd-2(del UBA)
W
icd-1(tm2873)
X
SQST-1::GFP
icd-1(tm2873)
Y
icd-1(tm2873); Picd-1::icd-1
Z
SQST-1::GFP
icd-1(tm2873); Picd-1::icd-1
A2
intestine
icd-2(RNAi); let-363(RNAi)
B2
SQST-1::GFP
icd-2(RNAi); let-363(RNAi)
C2
muscle
icd-2(RNAi)
D2
SQST-1::GFP
icd-2(RNAi)
E2
muscle
icd-2(RNAi); let-363(RNAi)
F2
SQST-1::GFP
icd-2(RNAi); let-363(RNAi)

Figure S1

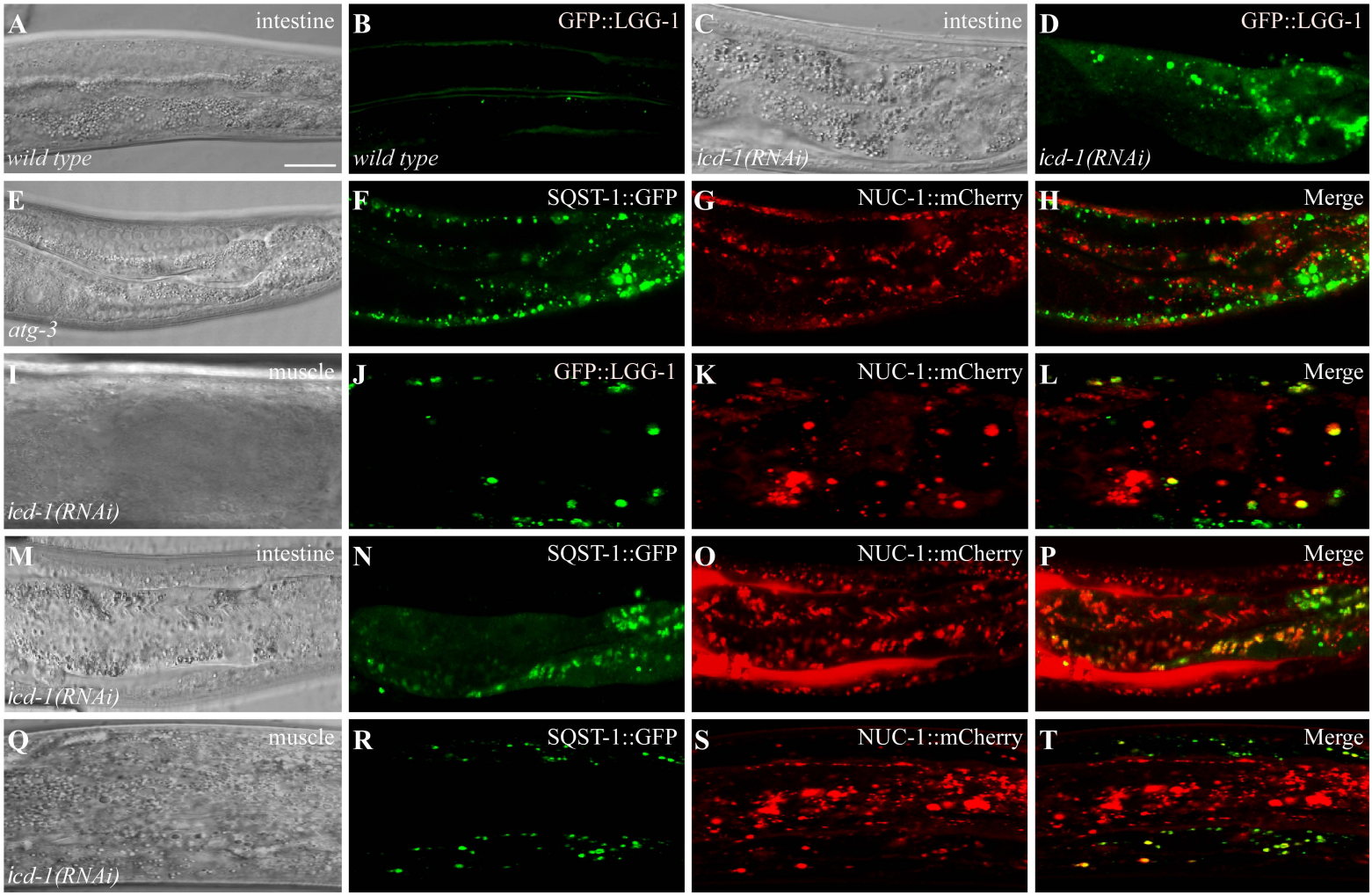
A
intestine
wild type
B
GFP::LGG-1
wild type
C
intestine
icd-1(RNAi)
D
GFP::LGG-1
icd-1(RNAi)
E
atg-3
F
SQST-1::GFP
G
NUC-1::mCherry
H
Merge
I
muscle
icd-1(RNAi)
J
GFP::LGG-1
K
NUC-1::mCherry
L
Merge
M
intestine
icd-1(RNAi)
N
SQST-1::GFP
O
NUC-1::mCherry
P
Merge
Q
muscle
icd-1(RNAi)
R
SQST-1::GFP
S
NUC-1::mCherry
T
Merge

Figure S2

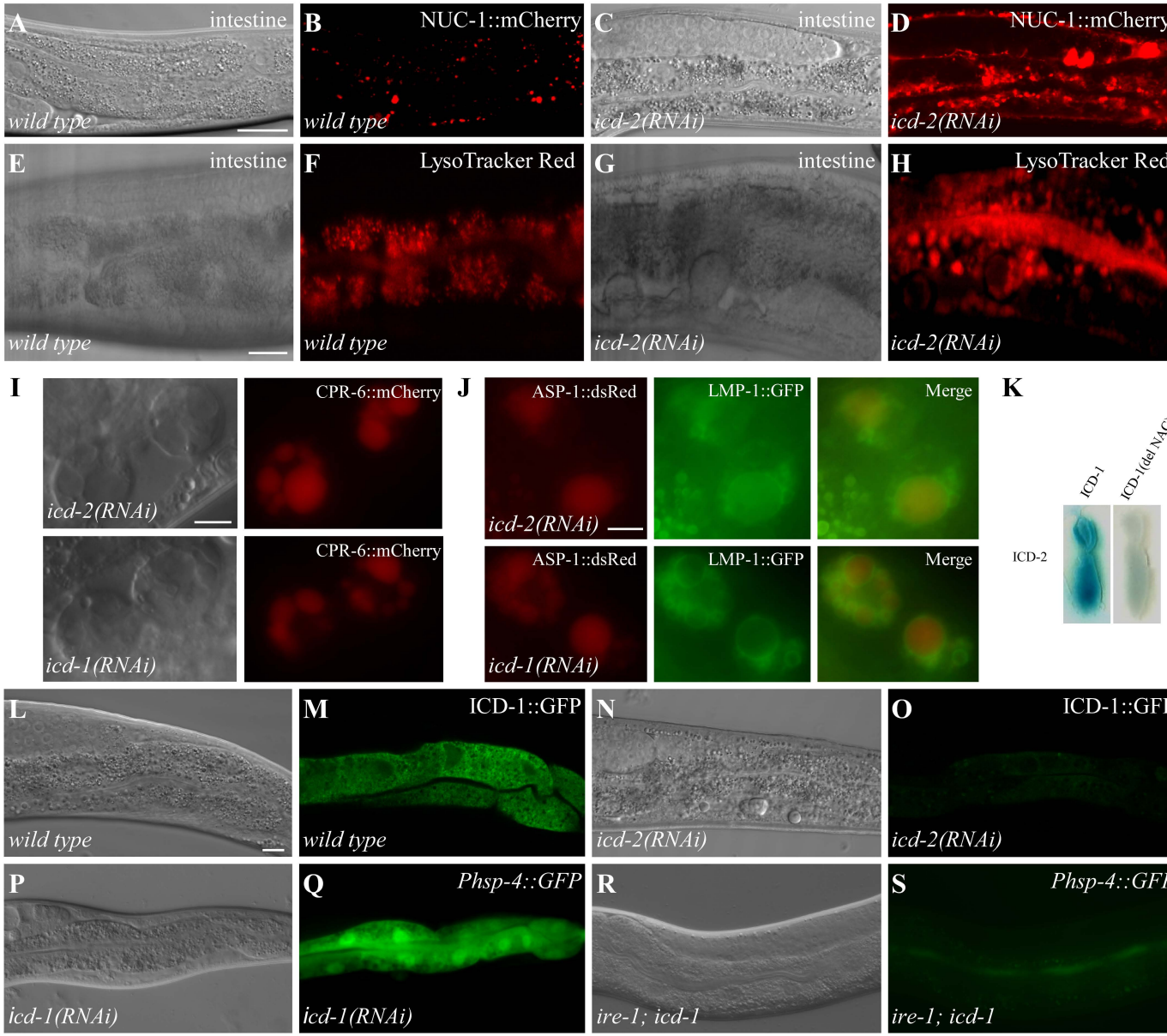
A
intestine
wild type
B
NUC-1::mCherry
wild type
C
intestine
icd-2(RNAi)
D
NUC-1::mCherry
icd-2(RNAi)
E
intestine
wild type
F
LysoTracker Red
wild type
G
intestine
icd-2(RNAi)
H
LysoTracker Red
icd-2(RNAi)
I
icd-2(RNAi)
CPR-6::mCherry
icd-1(RNAi)
CPR-6::mCherry
J
ASP-1::dsRed
LMP-1::GFP
Merge
icd-2(RNAi)
ASP-1::dsRed
LMP-1::GFP
Merge
icd-1(RNAi)
K
ICD-1
ICD-1(del NAC)
ICD-2
L
wild type
M
ICD-1::GFP
wild type
N
icd-2(RNAi)
O
ICD-1::GFP
icd-2(RNAi)
P
icd-1(RNAi)
Q
Phsp-4::GFP
icd-1(RNAi)
R
ire-1; icd-1
S
Phsp-4::GFP
ire-1; icd-1

Figure S3

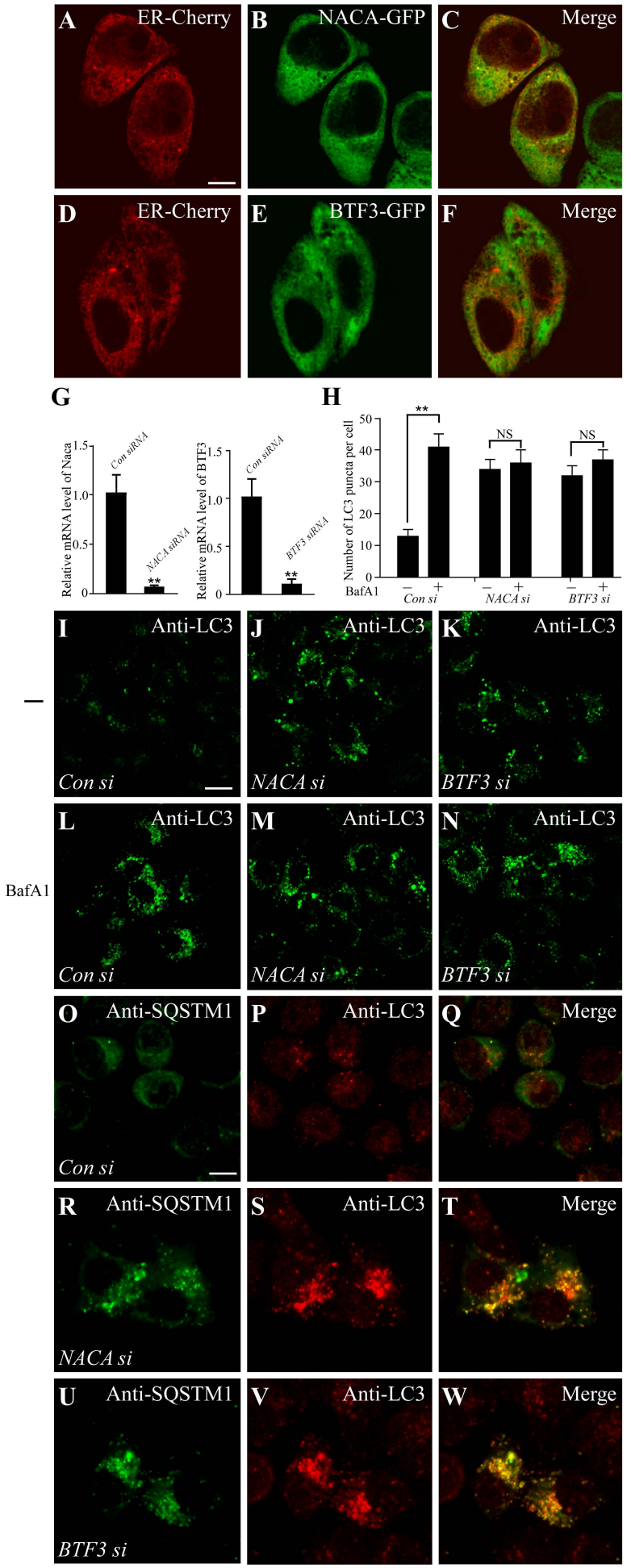
A ER-Cherry
B NACA-GFP
C Merge
D ER-Cherry
E BTF3-GFP
F Merge
G
Relative mRNA level of Naca
Con siRNA
NACA siRNA
**
Relative mRNA level of BTF3
Con siRNA
BTF3 siRNA
**
H
Number of LC3 puncta per cell
**
NS
NS
BafA1
Con si
NACA si
BTF3 si
I Anti-LC3
Con si
J Anti-LC3
NACA si
K Anti-LC3
BTF3 si
BafA1
L Anti-LC3
Con si
M Anti-LC3
NACA si
N Anti-LC3
BTF3 si
O Anti-SQSTM1
Con si
P Anti-LC3
Q Merge
R Anti-SQSTM1
NACA si
S Anti-LC3
T Merge
U Anti-SQSTM1
BTF3 si
V Anti-LC3
W Merge

Figure S4

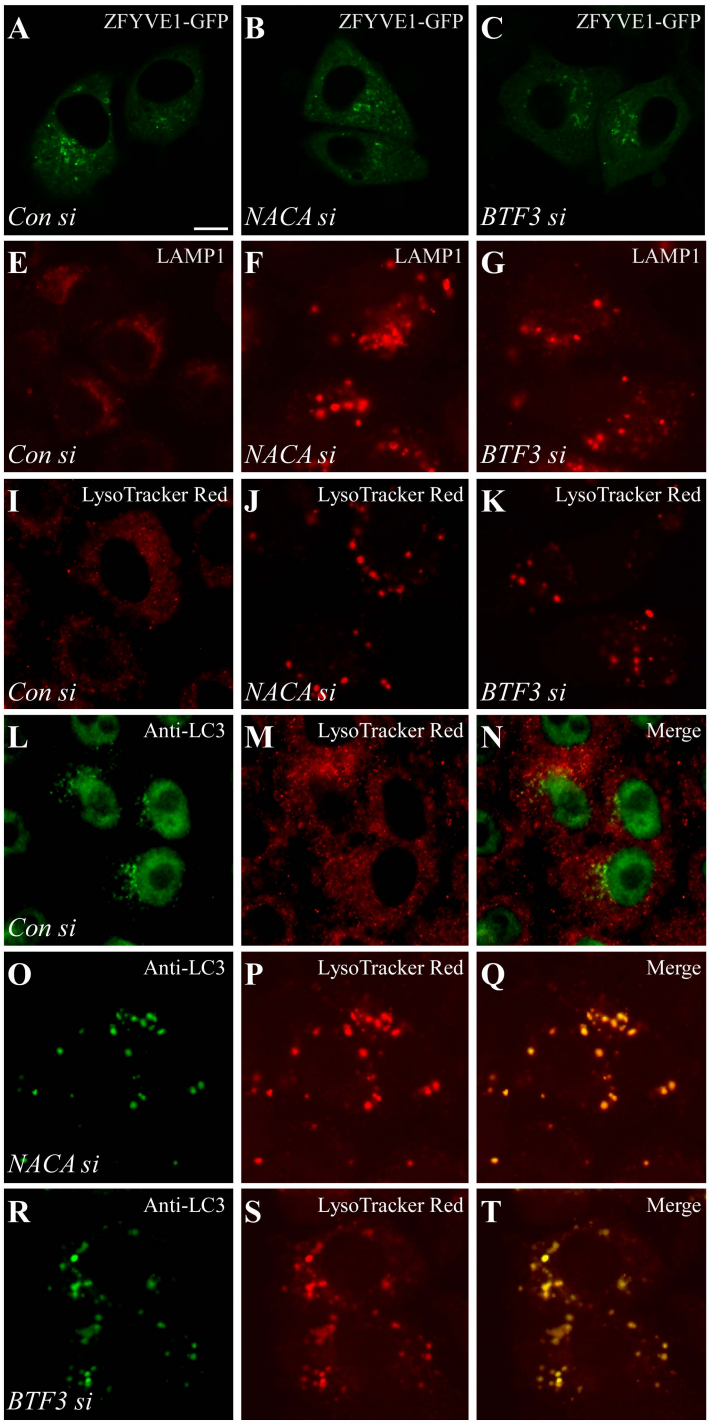
A ZFYVE1-GFP
Con si
B ZFYVE1-GFP
NACA si
C ZFYVE1-GFP
BTF3 si
E LAMP1
Con si
F LAMP1
NACA si
G LAMP1
BTF3 si
I LysoTracker Red
Con si
J LysoTracker Red
NACA si
K LysoTracker Red
BTF3 si
L Anti-LC3
Con si
M LysoTracker Red
N Merge
O Anti-LC3
NACA si
P LysoTracker Red
Q Merge
R Anti-LC3
BTF3 si
S LysoTracker Red
T Merge

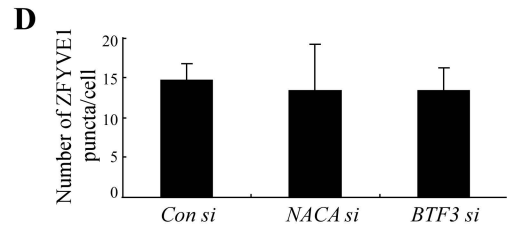
D
Number of ZFYVE1 puncta/cell
20
15
10
5
0
Con si
NACA si
BTF3 si

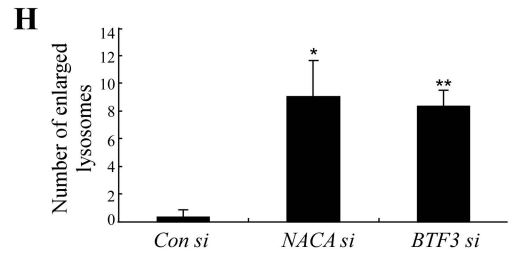
H
Number of enlarged lysosomes
14
12
10
8
6
4
2
0
*
**
Con si
NACA si
BTF3 si

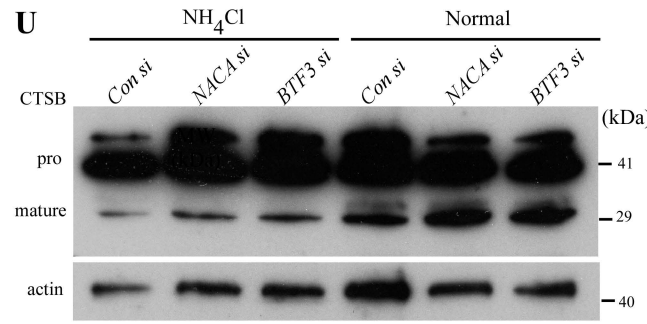
U
NH4Cl
Normal
Con si
NACA si
BTF3 si
Con si
NACA si
BTF3 si
CTSB
pro
mature
actin
(kDa)
41
29
40

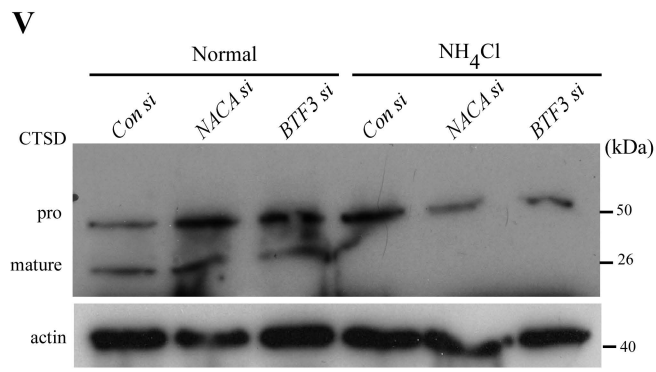
V
Normal
NH4Cl
Con si
NACA si
BTF3 si
Con si
NACA si
BTF3 si
CTSD
pro
mature
actin
(kDa)
50
26
40

Figure S5

Supplemental figure legends

Figure S1. Loss of function of *icd-2* and *icd-1* causes a defect in degradation of SQST-1 in *C. elegans.* (**A to D**) SQST-1::GFP accumulates into a large number of small spherical aggregates in the intestine in *bec-1(RNAi)* (**A and B**), *atg-7(RNAi)* (**C**) and *epg-5(RNAi)* (**D**) animals. (**E and F**) Endogenous SQST-1, detected by anti-SQST-1, is weakly expressed in intestine in wild-type animals. (**G to L**) Endogenous SQST-1 aggregates accumulate in the intestine in animals with RNAi inactivation of *lgg-1* (**G and H**), *vps-34* (**I and J**), *icd-2* (**K and L**). (**E**), (**G**), (**I**) and (**K**): DAPI images of the animals shown in (**F**), (**H**), (**J**) and (**L**), respectively. (**M and N**) SQST-1::GFP aggregates accumulate in the intestine in *icd-1(RNAi)* animals. (**O and P**) SQST-1::GFP aggregates accumulate in muscle cells in *icd-1(RNAi)* animals. (**Q to V**) *icd-2(tm3125)* mutants show accumulation of SQST-1::GFP aggregates in muscle and intestinal cells (**Q and R**). The defect is rescued by a transgene expressing ICD-2 (**S and T**) or by a transgene expressing mutant ICD-2 with a deletion of the UBA domain (**U and V**). (**W to Z**) Accumulation of SQST-1::GFP aggregates in *icd-1(tm2873)* mutants (**W and X**) is rescued by a transgene expressing *icd-1* (**Y and Z**). (**A2 and B2**) Accumulation of SQST-1::GFP aggregates in the intestine in *icd-2(RNAi)* animals is not suppressed by *let-363* inactivation. (**C2 to F2**) Accumulation of SQST-1::GFP aggregates in muscle cells in *icd-2(RNAi)* animals is not suppressed by inactivation of *let-363*. (**M**), (**O**), (**Q**), (**S**), (**U**), (**W**), (**Y**), (**A2**), (C2) and (**E2**): Nomarski images of the animals shown in (**N**), (**P**), (**R**), (**T**), (**V**), (**X**), (**Z**), (**B2**), (**D2**) and (**F2**), respectively. Scale bars: 20 μm. Young adult animals were

examined.

Figure S2. SQST-1 aggregates and GFP::LGG-1 puncta in *icd-1(RNAi)* animals colocalize with NUC-1::mCherry-labeled lysosomes. (**A and B**) GFP::LGG-1 is weakly expressed in the intestine in a wild-type animal. (**C and D**) GFP::LGG-1 forms a large number of puncta in the intestine in *icd-1(RNAi)* animals. (**A**) and (**C**): Nomarski images of the animals shown in (**B**) and (**D**), respectively. (**E to H**) SQST-1::GFP aggregates in the intestine in *atg-3* mutants are separable form NUC-1::mCherry-labeled lysosomes. (**I to L**) GFP::LGG-1 puncta in muscle cells in *icd-1(RNAi)* animals colocalize with NUC-1::mCherry. (**M to T**) SQST-1-GFP aggregates in the intestine (**M to P**) and muscle cells (**Q to T**) colocalize with NUC-1::mCherry-labeled lysosomes. (**E**), (**I**), (**M**) and (**Q**): Nomarski images of the animals shown in the same row. Scale bars: 20 μm. Young adult animals were examined.

Figure S3. Loss of function of NAC causes the accumulation of enlarged lysosomes. (**A to D**) Compared to wild-type intestine (**A and B**), NUC-1::mCherry-labeled lysosomal structures in the intestine are enlarged in *icd-2(RNAi)* animals (**C and D**). NUC-1::mCherry-labeled tubular lysosomes in the intestine are not obvious in young adult animals but become evident in older animals. (**E to H**) Compared to wild-type intestine (**E and F**), lysosomes stained by LysoTracker Red are enlarged in *icd-2(RNAi)* animals (**G and H**). (**I**) Enlarged lysosomes in coelomocytes in

icd-2(RNAi) and *icd-1(RNAi)* animals are labeled by CPR-6::mCherry. (**J**) ASP-1::dsRed labels the enlarged lysosomes, shown as LMP-1::GFP, in coelomocytes in *icd-2(RNAi)* and *icd-1(RNAi)* animals. (**K**) ICD-2 binds with ICD-1, but not with mutant ICD-1 with a deletion of the NAC domain, in a yeast two-hybrid analysis using an X-gal assay. (**L to O**) Compared to that in wild-type animals (**L and M**), the expression level of ICD-1::GFP is dramatically decreased in *icd-2(RNAi)* animals (**N and O**). (**P to S**) The elevated expression of *Phsp-4::GFP* in the intestine in *icd-1(RNAi)* animals (**P and Q**) is suppressed by simultaneous depletion of *ire-1* (**R and S**). (**A**), (**C**), (**E**), (**G**), (**L**), (**N**), (**P**) and (**R**): Nomarski images of the animals shown in (**B**), (**D**), (**F**), (**H**), (**M**), (**O**), (**Q**) and (**S**), respectively. Scale bars: 20 μm (**A to H, L to S**), 5 μm (**I and J**). Young adult animals were examined in (**A to D**) and (**L to S**). (**E to H**) show old adults. Animals in (**I and J**) were examined 24 h after the L4 stage.

Figure S4. Loss of function of NAC in mammalian cells causes a defect in the autophagy pathway. (**A to F**) NACA-GFP and BTF3-GFP colocalize with ER-Cherry in HeLa cells. (**G**) *NACA* and *BTF3* siRNA treatment greatly reduces levels of *NACA* and *BTF3* mRNA. ***P*<0.01. (**H**) Number of endogenous LC3 puncta in control (Con) siRNA, *NACA* siRNA or *BTF3* siRNA-treated cells with (+) or without (-) BafA1 treatment. Fifty cells were counted. ***P*<0.01. (**I to N**) Compared with Con siRNA-treated cells, the number of LC3 puncta, detected by anti-LC3, is increased in *NACA* and *BTF3* knockdown cells (**I to K**), but is not further increased after BafA1

treatment (**L to N**). (**O to W**) Compared to control cells, SQSTM1 aggregates dramatically accumulate and largely colocalize with LC3 puncta in *NACA* siRNA and *BTF3* siRNA-treated cells. Scale bars: 10 μm.

Figure S5. Loss of function of NAC causes accumulation of enlarged lysosomes. (**A to D**) Knockdown of *NACA* and *BTF3* does not affect the formation of ZFYVE1-GFP puncta. Numbers of ZFYVE1-GFP puncta are shown in (**D**). Thirty cells were counted. (**E to K**) Compared to control cells, lysosomes, labeled by LAMP1 (**E to G**) or detected by LysoTracker Red staining (**I to K**), are much larger in *NACA* and *BTF3* knockdown cells. (**H**) Numbers of enlarged lysosomes (with diameter larger than 1.5 μm) in control, *NACA* and *BTF3* knockdown cells. Fifty cells were counted. **P*<0.05, ***P*<0.01. (**L to T**) In *NACA* and *BTF3* knockdown cells, LC3 puncta, detected by anti-LC3, colocalize with enlarged lysosomes, detected by LysoTracker Red staining. (**U and V**) Maturation of CTSB and CTSD is not affected by *NACA* and *BTF3* knockdown. NH_4Cl treatment blocks maturation of CTSB and CTSD and thus serves as a positive control. Scale bars: 10 μm.